Identifying and comparing states of time-delayed systems: phase diagrams and applications to human movements

T.D. Frank[1], R. Friedrich[1], P.J. Beek[2]

Institute for Theoretical Physics, University of Münster, Wilhelm-Klemm-Str. 9, 48149 Münster, Germany

[2]*Faculty of Human Movement Sciences, Vrije Universiteit, Van der Boechorststraat 9, 1081 BT Amsterdam, The Netherlands*

Abstract

A data driven characterization of time-delayed stochastic systems is proposed in terms of linear delay differential equations and two drift parameters. It is shown how these parameters determine the states of such systems with respect to generalized phase diagrams. This approach allows for a comparison of systems with different system parameters as exemplified for two motor control tasks: tracking and force production.

PACS: 87.19.St, 02.30.Ks, 05.45.Tp

1 Introduction

The growing interdisciplinary interest in dynamical systems that involve time-delayed feedback loops [1–18] has inspired various attempts to derive evolution

[1] e-mail: tdfrank@uni-muenster.de

equations with delays from experimental data [19–23]. While the focus of most of these studies has been on time-delayed deterministic systems, a data analysis method designed for Markov diffusion processes [24,25] has recently been adopted in order to cope with time-delayed non-Markovian systems [26,27]. So far, emphasize has been placed on the derivation of the complete nonlinear dynamics of time-delayed systems. However, in many cases systems exhibit only small fluctuations around stationary fixed points and, consequently, can be regarded as linear systems driven by weak fluctuating forces. This important since ubiquitous special case has not yet been discussed in detail.

In the present study, we apply the data analysis method for time-delayed systems developed in [26,27] to linear systems and, in doing so, propose a description of the states of these systems in terms of two dynamical coefficients (a and b, see Sec. 2). By means of this approach, states can be related to phase transition lines and states of systems with different system parameters can be compared. Our general considerations will be illustrated for two motor control problems, namely, tracking and isometric force production (see Sec. 3).

2 Phase diagrams and states of stochastic time-delayed systems

2.1 Phase diagrams

We consider univariate stochastic systems involving a time delay τ and additive fluctuating forces ξ. We assume that the state variable $X(t)$, where t denotes time, is defined on a finite interval $\Omega = [x_{\min}, x_{\max}]$. We restrict our attention to stationary systems exhibiting stationary distribution $P_{\rm st}(x) = \langle \delta(x - X(t) \rangle_{\rm st}$. In line with our introductory remarks, there is a large class of systems exhibiting small fluctuations around a mean value. In these cases, we are dealing with unimodal distributions with standard deviations $\sigma \ll$

$x_{\max} - x_{\min}$. Let M_1 denote the mean of $P_{\rm st}(x)$. Then, for the sake of conveniency, we shift the state variable $X(t)$ by M_1 like $X(t) \to x(t) - M_1$ and thus obtain a random variable centered around zero. Accordingly, the linear stochastic delay-differential equation of the systems under consideration are given by

$$\frac{\mathrm{d}}{\mathrm{d}t}X(t) = aX(t) + bX(t-\tau) + \xi(t) \ . \tag{1}$$

The deterministic part involves two drift parameters a and b. As shown in the left panel of Fig. 1, these parameters determine for every τ the phase diagram of the time-delayed system.

Insert Fig. 1 about here

Figure 1 (left panel) depicts (in schematic fashion) the phase transition lines for two delays τ_1 and τ_2 with $\tau_2 > \tau_1$. There are two kinds of phase transition lines. The straight upper line is independent of τ and given by

$$b = -a \ , \tag{2}$$

whereas the curved lower line is defined by the parametric equation

$$a(t) = t\cot(\tau t) \ , \quad b(t) = -t/\sin(\tau t) \tag{3}$$

with $t \in (0, \pi/\tau)$ and $\lim_{t\to 0}(a,b) = (1/\tau, -1/\tau)$; for details see [28–30] and references therein. Obviously, there is an intersection point of both lines at $(a,b) = (1/\tau, -1/\tau)$. Let us dwell on the meaning of these phase transition lines for a moment.

For vanishing fluctuations, the phase transition lines correspond to bifurcation lines separating a stable and an unstable parameter regime. Here, stable (unstable) means that the fixed point $x = 0$ is a stable (unstable) solution of the evolution equation $\dot{x} = ax + bx(t-\tau)$ as predicted by linear stabil-

ity analysis. It can be shown that the bifurcation line $b = -a$ describes a non-oscillatory bifurcation (except for $a = \pm n\pi/(2\tau)$ and $n = 1, 2, 3, \ldots$), whereas the parametric bifurcation line describes a Hopf bifurcation with oscillation frequency $\omega_c = \sqrt{b^2 - a^2}$ [28–30]. Therefore, $(a, b) = (1/\tau, -1/\tau)$ is a co-dimension two-bifurcation point. In the presence of fluctuations, the phase transition lines demarcate the boundaries between two phases. In the stable regime stationary distributions exist, whereas in the unstable parameter regime such distributions do not exist. This results holds for a variety of fluctuating forces $\xi(t)$ ranging from Langevin forces to shot noise and Lévy noise fluctuating forces [31–36]. In sum, the phase transition lines separate stationary and non-stationary phases. The phase diagram of the time-delayed stochastic equation (1) may be regarded in the context of conventional phase diagrams of matter. For example, the right panel of Fig. 1 depicts schematically the phase diagram of a van der Waals gas. The phase transition lines (isotherms), which are drawn for two different temperatures T_1 and T_2 with $T_2 > T_1$ separate fluid and gas phases.

2.2 Identifying and comparing states

At this stage, we may pose two questions. First, how can the dynamical parameters a and b be determined from experimental data? Second, how can systems with different time delays be compared with each other in terms of a and b?

Identifying states

In general, the drift function $h(x, x_\tau)$ of time-delayed stochastic systems satisfying

$$\frac{\mathrm{d}}{\mathrm{d}t}X(t) = h(X, X_\tau) + \xi(t) \tag{4}$$

with $X_\tau = X(t-\tau)$ can be estimated by means of

$$h(x, x_\tau) \approx \frac{1}{\Delta t} \left(X(t+\Delta t) - X(t)\right)|_{X(t)=x, X(t-\tau)=x_\tau} \quad , \tag{5}$$

where Δt should be small (see [26,27] for $\xi(t)$ corresponding to a Langevin force and [37] for the general case). Note that the estimate (5) becomes exact in the limiting case $\Delta t \to 0$. Using Eq. (4), we obtain

$$a = \frac{\partial h(0,0)}{\partial x} \ , \quad b = \frac{\partial h(0,0)}{\partial x_\tau} \ . \tag{6}$$

Comparing states

It is well-known that Eq. (1) allows for a scaling procedure to eliminate the delay τ to a certain extent. Accordingly, we put $t = \tau t^*$ and introduce the new variables $X^*(t^*) = X(t)$ and $\xi^*(t^*) = \xi(t)$. Then, Eq. (1) can be transformed into

$$\frac{\mathrm{d}}{\mathrm{d}t^*} X^* = a^* X^*(t^*) + b^* X^*(t^* - 1) + \xi^*(t^*) \tag{7}$$

with

$$a^* = \tau a \ , \quad b^* = \tau b \ . \tag{8}$$

As a result, systems with arbitrary time delays τ can be mapped to systems with time delays $\tau = 1$. They can then be compared in terms of the re-scaled variables a^* and b^*. In other words, we propose a two-step procedure. First, the states of time-delayed stochastic system are determined from experimental data in terms of the parameters a and b using Eqs. (5) and (6). Second, the dynamical state variables a and b are re-scaled which gives us the new state variables a^* and b^*. Systems can then be compared in terms of their re-scaled state variables.

3 Applications

3.1 Tracking

3.1.1 Basics

Tracking is a fundamental example of coordinated human movement as well as of a man-machine system. Both coordinated movements [38–40] and man-machine systems [41] have attracted the interest of many scientists for various reasons. Tracking naturally involves time delays in terms of reaction time delays. In the following, however, we will consider a experimental setup introduced by Tass and colleagues [13,42] in which the time delay can be fixed by the experimenter and thus be manipulated.

Insert Fig. 2 about here

As shown in Fig. 2, a subject sits in front of a screen on which a moving target is displayed that oscillates with a frequency Ω. The subject is asked to track the target signal with the hand by performing oscillatory arm movements around the elbow. Vision of hand and arm is excluded. The hand position is displayed on the screen. Consequently, the subject needs to match the displayed hand position with the target signal. In order to manipulate the time delay involved in this man-machine interaction, the display of the hand position is retarded. That is, the signal displayed at time t corresponds to the hand position at time $t - \tau$; for further details see also [13].

Hand position and target signal can be described in terms of the time-dependent angular variables $\phi_h(t)$ and $\phi_t(t)$. The state variable of interest is the time-dependent relative phase defined by $\Delta\phi(t) = \phi_h(t) - \phi_t(t)$. In order to successfully perform the tracking task under time-delayed feedback the relative phase should satisfy $\Delta\phi \approx \tau\Omega$. Therefore, in what follows, we study the dynamics of the centered state variable $X(t) = \Delta\phi - \langle\Delta\phi\rangle \approx \Delta\phi(t) - \tau\Omega$. For

tracking movements exhibiting small fluctuations we assume that $X(t)$ satisfies the linear evolution equation (1) (see also [35]). The time delay τ in Eq. (1) roughly corresponds to the time delay of the feedback-display mechanism. Consequently, the parameter b measures the strength ($|b|$) and impact (sign of b) of the visual motor control mechanism. In contrast, a is assumed to reflect the strength and impact of a non-delayed motor control mechanism, the so-called proprioceptive control [13,35].

3.1.2 Results

We report here data from three subjects that performed the tracking task with $\max\{|\langle\Delta\phi\rangle - \tau\Omega|\} < 0.1$. That is, they successfully participated in the experiments. The standard deviation was of the order of magnitude of 10^{-1}. Recall that we have $\Delta\phi \in [0, 2\pi]$. Consequently, we have $\sigma \ll 2\pi$. That is, the performed tracking movements exhibited only relatively small fluctuations. All subjects performed tracking movements at three different frequencies Ω and under two time delays denoted here τ_h (high) and τ_l (low) with $\tau_h > \tau_l$ (the exact τ-values were subject-dependent in order to account for preferred tracking frequencies [13]). Data were recorded at 1000 Hz and down sampled to 100 Hz in order to eliminate digitalization noise. For every condition the parameters a and b were determined from the experimental data using time-averaging and Eqs. (5) and (6). The re-scaled parameters a^* and b^* were computed from Eq. (8). The thus obtained variables a^* and b^* are shown in the phase diagram depicted in Fig. 3.

Insert Fig. 3 about here

We appreciate from this figure that the states are closer to the phase transition line $b = -a$ than to the parametric phase transition line. We conclude that the motor control systems operate closer to the non-oscillatory bifurcation line than to the oscillatory bifurcation line. Note that in the context of tracking movements the two phase transition lines can be interpreted in a specific sense.

The line $b = -a$ means that at the instability point the relative phase grows exponentially. This exponential increase will stop at large amplitudes when nonlinearities of the system dynamics become relevant. As a result, we expect that the relative phase at the non-oscillilatory instability will perform a phase slipping movement. In contrast, at the Hopf instability line the relative phase will start to oscillate with the Hopf frequency ω_c. That is, our analysis reveals that depending on where the parameters a^* and b^* cross the phase transition lines we will observe either phase slipping or phase oscillations, see Fig. 4. In fact, in previous experiments both kinds of instabilities have been observed [13].

Insert Fig. 4 about here

Let us now discuss the impact (sign of a^*, b^*) and strength ($|a^*|$, $|b^*|$) of the control mechanisms involved in the tracking tasks. From Fig. 3 we see that in all cases $b^* < 0$ and in all but one case $a^* > 0$. In line with our interpretation of the parameters a^* and b^*, we conclude that the visual motor control system corresponds to a negative feedback loop that yields a stabilization of the required fixed point, whereas the proprioceptive control de-stabilizes the system. In order to evaluate the magnitude of the parameters a^* and b^* we compare states variables a^* and b^* corresponding to different time delays, see Fig. 5.

Insert Fig. 5 about here

We see that in all cases $|b^*|$ increases with increasing time delay. This means that the role of the visual motor control system becomes more important for larger time delays. In contrast, we found no clear tendency for the parameter a^*.

3.2 Isometric force production

3.2.1 Basics

When muscles produce forces without changing length the produced force is called isometric. The study of isometric force production has led to many insights into force production in general [43,44]. In what follows, we will use the data analysis method outlined in Sec. 2 in order to identify passive and active parts of motor control systems involved in isometric force production.

Insert Fig. 6 about here

Isometric forces produced by index fingers can be measures by means of an experimental setup shown in Fig. 6. Here, a subject is seated in front of a screen with the right forearm on a pad. The fingertip of the index finger of the right hand is placed on the surface of a force transducer. A horizontal bar (dashed line in Fig. 6) indicates the required force. A second horizontal bar (solid line in Fig. 6) indicates the amount of force that is actually produced when the participant presses on the sensor. That is, while the first bar is immobile, the second bar can move in the vertical direction depending on the force applied to the force transductor.

Let $f(t)$ denote the force produced by a subject. It is useful to relate this force to the maximum voluntary force (MVF) of the subject such that the relative force is defined by $f_{\rm rel}(t) = f(t)/\mathrm{MVF}$. That is, $f_{\rm rel}(t)$ is the force $f(t)$ expressed as percentage of the maximal voluntary force. Similarly, the required force level $f_{\rm req}$ is defined in terms of the MVF (e.g. $f_{\rm req} = 0.2$ means 20% of the MVF). The force production task can then be described in terms of the state variable $X(t) = f_{\rm rel} - f_{\rm req}$ which indexes the deviation from the required force. For force production tasks exhibiting only small deviations, we assume that $X(t)$ satisfies Eq. (1). This means that we need to interpret the parameters a, b, τ of Eq. (1) in the context of isometric force production. Motor control sys-

tems in general typically involve neurophysiological (electromechanical) time delays τ in the range of 10...100 ms [15]. The relevant time delay is often determined by means of correlation and cross-correlation functions [15]. In order to stress our description of the motor control system as a dynamical system, where changes of state variables are related to the state variables themselves, we use the cross-correlation function $C(\tau) = \left\langle \dot{X}(t)X(t-\tau) \right\rangle$ and estimate τ from the first minimum of $C(\tau)$. From Eq. (1) we read off that the parameter b reflects the strength and impact of the active motor control loop involving the neurophysiological time delay τ. In contrast, the parameter a is related to an instantaneous response mechanism that acts on time scales at which active control is impossible. For example, a may reflect passive biomechanical properties. In short, we assume that a describes passive response properties involved in isometric force production.

3.2.2 Results

We report here data from seven subjects that participated successfully in the force production experiment with $\langle f_{\rm rel}(t) \rangle \approx f_{\rm req}$. The standard deviations of $X(t)$ were in the range between 0.01 (low force) and 0.05 (large force). Note that we have $X(t) \in [0, 1]$. Consequently, there were only small fluctuations around the required force level and the relation $\sigma \ll 1$ holds. In what follows we focus on three force levels (0.2, 0.4, and 0.6). The delay estimates gave us τ-values in the range of $[20, 30]$ ms for five subjects. For the remaining two subjects we found $\tau = 40$ ms and $\tau = 80$ ms. For all subjects and force levels the parameters a and b were determined and re-scaled. The state variables a^* and b^* are depicted in Fig. 7.

Insert Fig. 7 about here

On the average, the states are distributed closer to the phase transition line $b = -a$ than to the parametric phase transition line. Evaluating the signs of a^* and b^*, we found in all cases that b^* is negative. In most cases a^* was positive. This result illustrates that stable performance is primarily due to

the active motor control loop — which is of course what one would expect. The passive motor control loop tends to de-stabilize the system. Regarding the magnitudes of the parameters a^* and b^*, we focused on the increments between different force levels. The increment vectors $(\Delta a_l^*, \Delta b_l^*)$ for the low force conditions and $(\Delta a_h^*, \Delta b_h^*)$ for the high force conditions were computed from $\Delta a_l^* = a^*(0.4) - a^*(0.2)$, $\Delta b_l^* = b^*(0.4) - b^*(0.2)$, $\Delta a_h^* = a^*(0.6) - a^*(0.4)$, and $\Delta b_h^* = a^*(0.6) - a^*(0.4)$. The results are shown in Fig. 8. We see that in all cases $|b^*|$ increases when the force level increases. This means that the active control loop becomes more important (or more stiff) when larger forces are produced. In contrast, there is no clear tendency of the parameter a^*.

Insert Fig. 8 about here

4 Conclusions

We studied time-delayed stochastic systems in terms of linearized evolution equations involving two drift parameters. We showed that these parameter can be determined from experimental data using a new, two-step data analysis method. We proposed to interpret the two drift parameters as state variables that characterize time-delayed stochastic systems with respect to phase diagrams of a particular kind. These phase diagrams, in turn, exhibit non-oscillatory and oscillatory instability lines that connect non-stationary and stationary phases. We exploited this phase diagram approach in order to study human motor control systems.

We reported data from two experiments on tracking and isometric force production. In both experiments motor control systems were found to operate closer to non-oscillatory phase transition lines than to oscillatory ones. Therefore, we may speculate that the first instabilities that will be observed in these systems will be non-oscillatory instabilities such as phase slipping in the case of tracking or a force breakdown in the case of the isometric force production.

Furthermore, we found that the active time-delayed motor control mechanisms gain importance (or become more stiff) when time delays increase (tracking) and when higher forces have to be produced (force production). In other words, our analysis illustrates qualitatively that the active time-delayed motor control feedback loops become more important when motor control tasks become more complicated — which is a statement that appeals to our intuition.

References

[1] R. Lang and K. Kobayashi, IEEE J. Quantum Electron. **16**, 347 (1980).

[2] E. Villermaux, Phys. Rev. Lett. **75**, 4618 (1995).

[3] L. S. Tsimring and A. Pikovsky, Phys. Rev. Lett. **87**, 250602 (2001).

[4] C. Masoller, Phys. Rev. Lett. **90**, 020601 (2003).

[5] T. Ohira and Y. Sato, Phys. Rev. Lett. **82**, 2811 (1999).

[6] S. Kim, S. H. Park, and H. Pyo, Phys. Rev. Lett. **82**, 1620 (1999).

[7] J. M. Cushing, *Integrodifferential equations and delay models in population dynamics* (Springer, Berlin, 1977).

[8] M. C. Mackey and L. Glass, Science **197**, 287 (1977).

[9] Y. Chen, M. Ding, and J. A. S. Kelso, Phys. Rev. Lett. **79**, 4501 (1997).

[10] H. Haken, *Brain dynamics* (Springer, Berlin, 2002).

[11] A. Longtin, J. G. Milton, J. E. Bos, and M. C. Mackey, Phys. Rev. A **41**, 6992 (1990).

[12] K. Vasilakov and A. Beuter, J. Theo. Biol. **165**, 389 (1993).

[13] P. Tass, J. Kurths, M. G. Rosenblum, G. Guasti, and H. Hefter, Phys. Rev. E **54**, R2224 (1996).

[14] M. Schanz and A. Pelster, Phys. Rev. E **67**, 056205 (2003).

[15] J. L. Cabrera and J. G. Milton, Phys. Rev. Lett. **89**, 158702 (2002).

[16] G. A. Bocharov and F. A. Rihan, J. Comput. Appl. Math. **125**, 183 (2000).

[17] M. G. Rosenblum and A. S. Pikovsky, Phys. Rev. Lett. **92**, 114102 (2004).

[18] V. K. Jirsa and M. Ding, Phys. Rev. Lett. **93**, 070602 (2004).

[19] M. J. Bünner, M. Ciofini, A. Giaquinta, R. Hegger, R. Kantz, R. Meucci, and A. Politi, Eur. Phys. J. B **10**, 165 (2000).

[20] M. J. Bünner, T. Meyer, A. Kittel, and J. Parisi, Phys. Rev. E **56**, 5083 (1997).

[21] R. Hegger, M. J. Bünner, and H. Kantz, Rev. Phys. Lett. **81**, 558 (1998).

[22] W. Horbelt, J. Timmer, and H. U. Voss, Phys. Lett. A **299**, 513 (2002).

[23] V. I. Ponomarenko and M. D. Prokhorov, Phys. Rev. E **66**, 026215 (2002).

[24] R. Friedrich and J. Peinke, Phys. Rev. Lett. **78**, 863 (1997).

[25] S. Siegert, R. Friedrich, and J. Peinke, Phys. Lett. A **243**, 275 (1998).

[26] T. D. Frank, P. J. Beek, and R. Friedrich, Phys. Rev. E **68**, 021912 (2003).

[27] T. D. Frank, P. J. Beek, and R. Friedrich, Phys. Lett. A **328**, 219 (2004).

[28] N. S. Goel, S. C. Maitra, and E. W. Montroll, Rev. Mod. Phys. **43**, 231 (1971).

[29] R. D. Driver, *Ordinary and delay differential equations — Applied mathematical sciences Vol. 20* (Springer, New York, 1977).

[30] J. Hale, *Theory of functional differential equations* (Springer, Berlin, 1977).

[31] U. Küchler and B. Mensch, Stochastics and stochastic reports **40**, 23 (1992).

[32] A. A. Gushchin and U. Küchler, Stoch. Proc. Appl. **88**, 195 (2000).

[33] A. A. Budini and M. O. Careres, Phys. Rev. E **70**, 046104 (2004).

[34] M. C. Mackey and I. G. Nechaeva, Phys. Rev. E **52**, 3366 (1995).

[35] T. D. Frank and P. J. Beek, Phys. Rev. E **64**, 021917 (2001).

[36] E. I. Verreist, in *Advances in time-delay systems*, edited by T. J. Barth, M. Griebel, D. E. Keyes, R. M. Nieminen, D. Roose, and T. Schlick (Springer, Berlin, 2004), pp. 390–420.

[37] T. D. Frank, R. Friedrich, and P. J. Beek, Stochastics and Dynamics, (2005), Time series analysis for multivariate time-delayed systems with noise: applications to laser physics and human movements, in press.

[38] M. T. Turvey, Am. Psychol. **45**, 938 (1990).

[39] P. J. Beek, C. E. Peper, and D. F. Stegeman, Hum. Movement Sci. **14**, 573 (1995).

[40] J. A. S. Kelso, *Dynamic patterns - The self-organization of brain and behavior* (MIT Press, Cambridge, 1995).

[41] K. U. Smith, *Delayed sensory feedback and behavior* (W. B. Saunders Company, Philadelphia, 1962).

[42] U. Langenberger, H. Hefter, K. R. Kessler, and J. D. Crooke, Exp. Brain Res. **118**, 161 (1998).

[43] K. M. Newell and D. M. Corcos, *Variability and motor control* (Human Kinetics Publishers, Champaign, 1993).

[44] A. B. Slifkin and K. M. Newell, J. Exp. Psychol. - Hum. Percept. Perform. **25**, 837 (1999).

Figure captions

Fig. 1: Phase diagrams of a time-delayed stochastic system (left panel) and a van der Waals gas (right panel).

Fig. 2: Experimental setup of the tracking task experiment with time-delayed visual feedback.

Fig. 3: Scatterplot of the re-scaled states given in terms of the parameters a^* and b^* found in different trials of the tracking experiment. Phase transition lines are computed from Eqs. (2) and (3) for $\tau = 1$.

Fig. 4: Illustration of two kinds of instabilities that might occur in tracking tasks: phase slipping instability (upper bifurcation line) and phase oscillation instability (lower bifurcation line).

Fig. 5: Comparison of state variables b^* for small and large time-delays (lines connect state variables belong to the same trial). $|b^*|$ increases when the time-delay is increased.

Fig. 6: Experimental setup of the isometric force production experiment.

Fig. 7: Scatterplot of the re-scaled states described by the dynamical parameters a^* and b^* found in different trials of isometric force production.

Fig. 8: Comparison of state variables b^* for different force levels of isometric force production (lines connect state variables belong to the same trial). $|b^*|$ increases when the force level is increased.

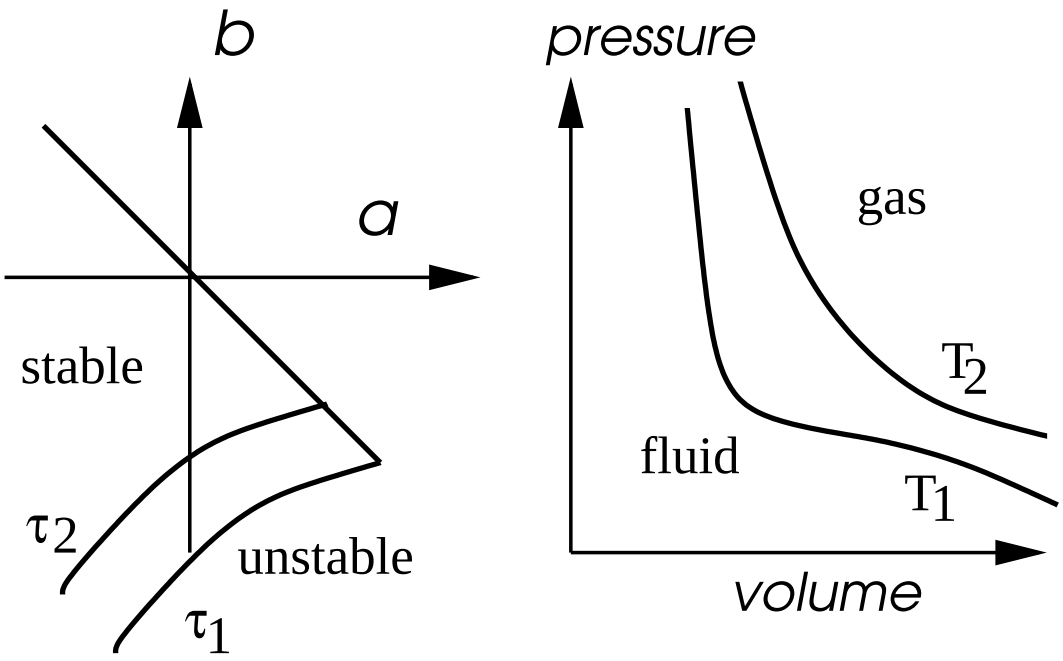

Fig. 1. Phase diagrams of a time-delayed stochastic system (left panel) and a van der Waals gas (right panel).

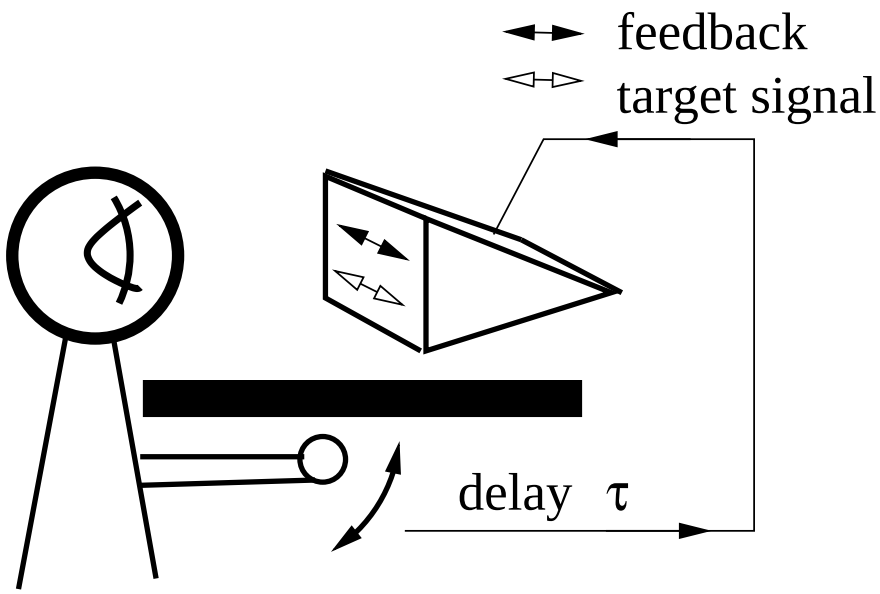

Fig. 2. Experimental setup of the tracking task experiment with time-delayed visual feedback.

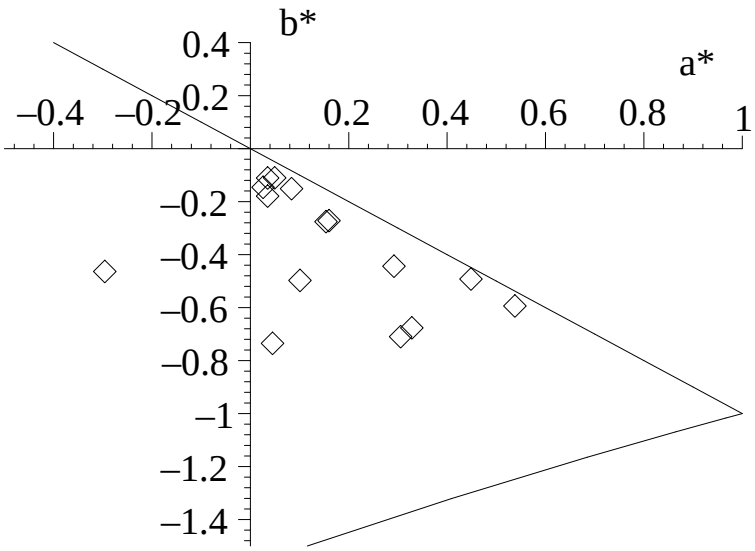

Fig. 3. Scatterplot of the re-scaled states given in terms of the parameters a^* and b^* found in different trials of the tracking experiment. Phase transition lines are computed from Eqs. (2) and (3) for $\tau = 1$.

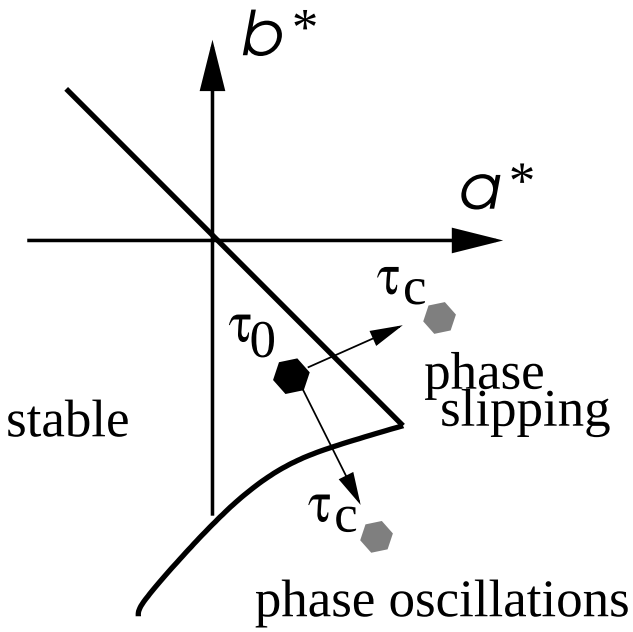

Fig. 4. Illustration of two kinds of instabilities that might occur in tracking tasks: phase slipping instability (upper bifurcation line) and phase oscillation instability (lower bifurcation line).

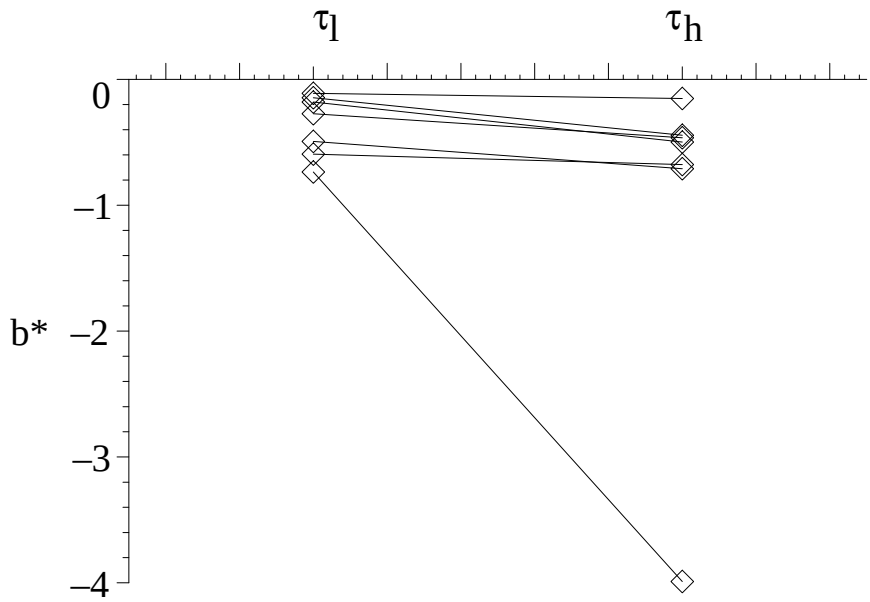

Fig. 5. Comparison of state variables b^* for small and large time-delays (lines connect state variables belong to the same trial). $|b^*|$ increases when the time-delay is increased.

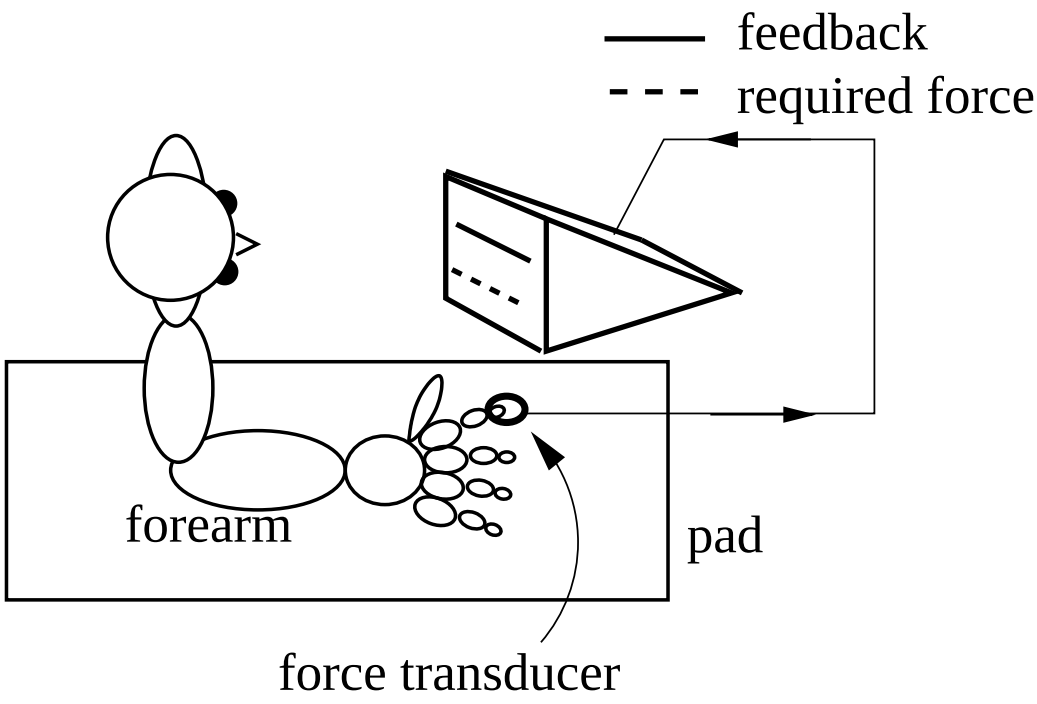

Fig. 6. Experimental setup of the isometric force production experiment.

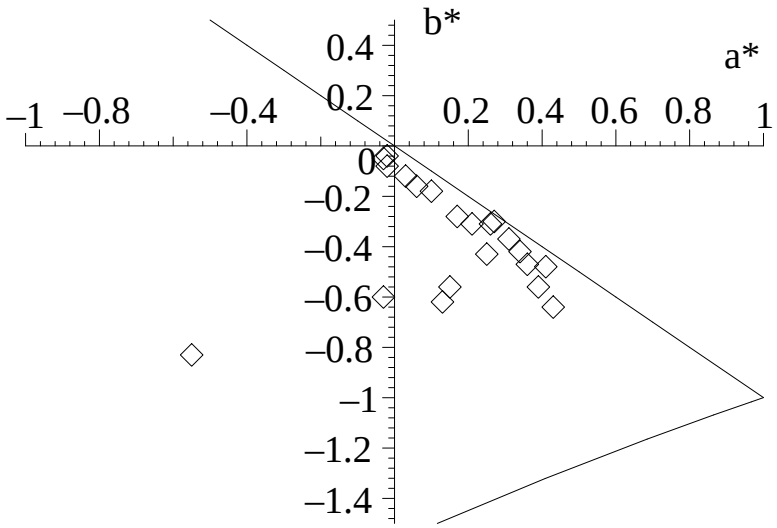

Fig. 7. Scatterplot of the re-scaled states described by the dynamical parameters a^* and b^* found in different trials of isometric force production.

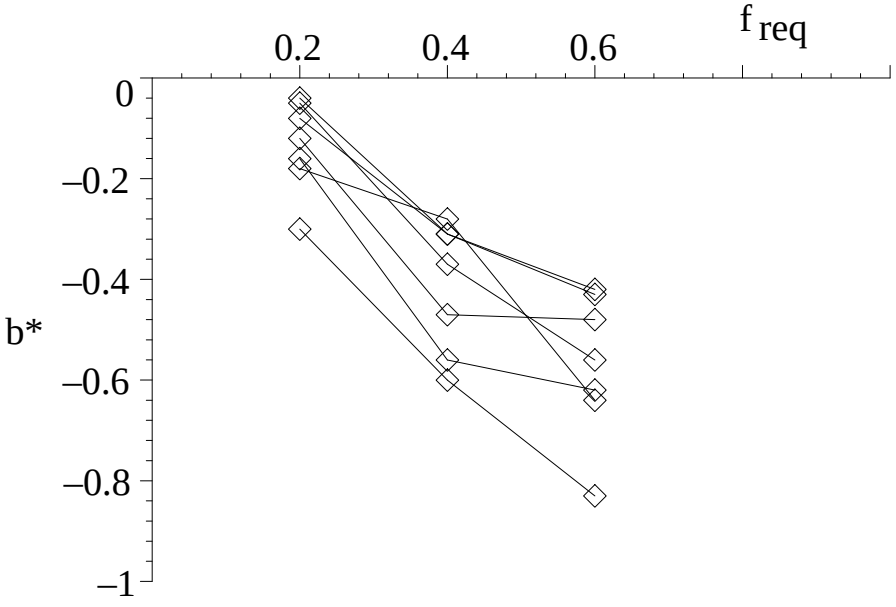

Fig. 8. Comparison of state variables b^* for different force levels of isometric force production (lines connect state variables belong to the same trial). $|b^*|$ increases when the force level is increased.